General Disclaimer

One or more of the Following Statements may affect this Document

- This document has been reproduced from the best copy furnished by the organizational source. It is being released in the interest of making available as much information as possible.

- This document may contain data, which exceeds the sheet parameters. It was furnished in this condition by the organizational source and is the best copy available.

- This document may contain tone-on-tone or color graphs, charts and/or pictures, which have been reproduced in black and white.

- This document is paginated as submitted by the original source.

- Portions of this document are not fully legible due to the historical nature of some of the material. However, it is the best reproduction available from the original submission.

Produced by the NASA Center for Aerospace Information (CASI)

NASA CR-135228

HYDRODYNAMIC EFFECTS IN A MISALIGNED RADIAL FACE SEAL

I. Etsion

Technion - Israel Institute of Technology
Haifa, Israel

(NASA-CR-135228) HYDRODYNAMIC EFFECTS IN A   N79-17226
MISALIGNED RADIAL FACE SEAL Final Report
(Israel Inst. of Tech.) 38 p HC A03/MF A01
                                    CSCL 11A   Unclas
                                            G3/37   35078

MAR 1979
RECEIVED
NASA STI FACILITY
AII BRANCH

Prepared for

NATIONAL AERONAUTICS AND SPACE ADMINISTRATION
Lewis Research Center
Cleveland, Ohio 44135

July 1977

1. Report No. NASA CR-135228	2. Government Accession No.	3. Recipient's Catalog No.
4. Title and Subtitle HYDRODYNAMIC EFFECTS IN A MISALIGNED RADIAL FACE SEAL		5. Report Date July 1977
		6. Performing Organization Code
7. Author(s) I. Etsion		8. Performing Organization Report No. None
		10. Work Unit No.
9. Performing Organization Name and Address Technion - Israel Institute of Technology Haifa, Israel		11. Contract or Grant No. NSG-7317
		13. Type of Report and Period Covered Contractor Report
12. Sponsoring Agency Name and Address National Aeronautics and Space Administration Washington, D.C. 20546		14. Sponsoring Agency Code
15. Supplementary Notes Final report. Project Manager, Lawrence P. Ludwig, Fluid System Components Division, NASA Lewis Research Center, Cleveland, Ohio 44135		

16. Abstract

Hydrodynamic effects in a flat seal having an angular misalignment are analyzed, taking into account the radial variation in seal clearance. An analytical solution for axial force, restoring moment, and transverse moment is presented that covers the whole range from zero to full angular misalignment. Both low pressure seals with cavitating flow and high pressure seals with full fluid film are considered. Strong coupling is demonstrated between angular misalignment and transverse moment which leads the misalignment vector by 90 degrees. This transverse moment, which is entirely due to hydrodynamic effects, is a significant factor in the seal operating mechanism.

17. Key Words (Suggested by Author(s)) Face seal; Radial face seal; Mechanical seal; Shaft seal	18. Distribution Statement Unclassified - unlimited STAR Category 37		
19. Security Classif. (of this report) Unclassified	20. Security Classif. (of this page) Unclassified	21. No. of Pages 37	22. Price*

NOMENCLATURE

C   - seal clearance along centerline

F   - axial force

$\overline{F}$ - nondimensional force, $F/6\mu\omega(r_0/C)^2 r_0^2$

h   - film thickness

I_1, I_2 - integrals defined in Eqs. (21) and (22)

I_3, I_4 - integrals defined in Eqs. (36) and (37)

J_1 - given by Eq. (26)

J_2 - given by Eq. (41)

M_x - restoring moment

$\overline{M}_x$ - nondimensional moment, $M_x/6\mu\omega(r_0/C)^2 r_0^3$

M_z - transverse moment

$\overline{M}_z$ - nondimensional moment, $M_z/6\mu\omega(r_0/C)^2 r_0^3$

p   - pressure

R   - nondimensional radius, r/r_0

r   - radial coordinate

r'   - radial coordinate of extreme pressure

x,z   - orthogonal axes, see Figure 1

Greek Symbols:

γ - angle of tilt

ε - tilt parameters, $\gamma r_0/C$

θ - angular coordinate

μ - viscosity

ω - rotational angular velocity

Subscripts:

ap   - approximate

i   - at inner radius

m   - at midradius

o   - at outer radius

INTRODUCTION

Seal leakage and short seal life are common problems found in a host of industrial equipment and in other applications. For this reason seal research has been carried out since the early sixties in an attempt to understand the mechanism of seal operation. Denny [1] has shown experimentally that hydrodynamic effects in a misaligned radial face seal are the cause for axial forces and pressures in excess of those theoretically predicted for aligned flat seal faces. Following Denny's findings, many investigators have treated this problem and there have been several hypotheses put forth to explain the mechanisms responsible for the development of the lubricating film pressure that acts to separate the primary seal faces. These hypotheses include surface angular misalignment [2], surface waviness [3,4,5], microasperities [6], vaporization of the fluid film [7], and thermal deformation [8,9]. Examination reveals that these theories are of limited use from an operation prediction standpoint, and that face seal lubrication theory is still very primitive. It is also noted that seal dynamics, which is thought to be of major importance, is poorly understood.

In some recent papers [10,11] an attempt is made to solve analytically the dynamic behavior of a radial face seal. In these papers the dynamic response of an angular misaligned seal is considered due to a restoring moment that coincides with the angular misalignment vector. This restoring moment, which is an important factor in seal stability, is by no means the only moment acting on the seal faces, a fact that somehow was overlooked in the past. A transverse moment that leads the angular misalignment vector by 90 degrees and is generated by hydrodynamic effects is pointed out in [12]. This

1

transverse moment may be the origin of dynamic instability and has to be considered in any dynamic analysis of a realistic seal model.

In order to establish a better understanding of radial face seal mechanism of operation, it is important to obtain the complete system of forces and moments. As a first step the hydrostatic effects in a misaligned seal were analyzed [12] and both the axial force and tilting moment were found. In this paper the hydrodynamic components of the forces and moments will be treated.

In previous works analytical results were limited to very small angular tilts [2], or to an approximated film thickness geometry where radial variations were neglected [11]. Also the transverse moment, mentioned before, was overlooked.

It is the objective of this paper to present an analytical solution for the hydrodynamic effects in a realistic misaligned seal geometry. This solution covers the complete range of seal misalignment from parallel faces to surface touch down.

ANALYSIS

The Reynolds equation for a narrow seal and incompressible fluid is:

$$\frac{\partial}{\partial r}\left(rh^3 \frac{\partial p}{\partial r}\right) = 6\mu\omega r \frac{\partial h}{\partial \theta} \tag{1}$$

where the film thickness, h, for a misaligned seal (Figure 1) is given by:

$$h = C + \gamma r\cos\theta \tag{2}$$

It is shown in [12] that while curvature effects may be neglected, thus allowing the replacement of r in (1) by the mean radius r_m, the film thickness in (2) should remain a function of both r and θ. This is due to the fact that the pressure is strongly affected by radial changes in the film thickness along the narrow width of the sealing gap.

In contrast to the film thickness, its circumferential gradient is almost unaffected by the radius and hence may be approximated by

$$\frac{\partial h}{\partial \theta} = -\gamma r_m \sin\theta$$

Eq. (1) then becomes

$$\frac{\partial}{\partial r}\left(h^3 \frac{\partial p}{\partial r}\right) = -6\mu\omega\gamma r_m \sin\theta \tag{3}$$

Integrating once we have

$$\frac{\partial p}{\partial r} = -\frac{6\mu\omega}{h^3}\gamma r_m \sin\theta(r-r') \tag{4}$$

where r' is a constant of integration corresponding to the radius where the pressure has an extremum. Integrating once again gives

$$p = - 6\mu\omega\gamma r_m \sin\theta \left[\frac{1}{\gamma^2 \cos^2\theta}\left(- \frac{1}{h} + \frac{C}{2h^2}\right) + \frac{r'}{2\gamma h^2 \cos\theta} \right] + C_1 \qquad (5)$$

with C_1 as another constant of integration. The boundary conditions for the hydrodynamic case are $p=0$ at $r=r_o$ and at $r=r_i$. Hence

$$\frac{1}{\gamma\cos\theta}\left(\frac{C}{2h_i^2} - \frac{1}{h_i}\right) + \frac{r'}{2h_i^2} = \frac{1}{\gamma\cos\theta}\left(\frac{C}{2h_o^2} - \frac{1}{h_o}\right) + \frac{r'}{2h_o^2}$$

or

$$r' = \frac{1}{\gamma\cos\theta}\left(2\frac{h_o h_i}{h_o + h_i} - C\right) \qquad (6)$$

Since

$$h_o h_i = C^2 + C\gamma(r_o + r_i)\cos\theta + \gamma^2 r_o r_i \cos^2\theta$$

and

$$C(h_o + h_i) = 2C^2 + C\gamma(r_o + r_i)\cos\theta$$

we get from (6)

$$r' = -\frac{C(r_o + r_i) + 2\gamma r_o r_i \cos\theta}{2C + \gamma(r_o + r_i)\cos\theta}$$

or in dimensionless form

$$R' = \frac{R_m + \epsilon R_i \cos\theta}{1 + \epsilon R_m \cos\theta} \qquad (7)$$

where $R = r/r_o$, $\epsilon = \gamma r_o/C$, and $R_m = (1+R_i)/2$.

Eq. (7) gives the radius where the radial pressure profile reaches its maximum or minimum. This radius clearly differs from the mean radius R_m at which the maximum pressure is obtained when radial variation in h are neglected [11].

The constant C_1 in Eq. (5) is found by equating p to zero at $r=r_o$. Thus the pressure distribution is

$$p = \frac{6\mu\omega r_m}{\gamma} \frac{\sin\theta}{\cos^2\theta} \frac{h-h_o}{h^2 h_o^2} [\frac{h_o+h}{2}(C + \gamma r'\cos\theta) - hh_o] \qquad (8)$$

From (6) we have

$$C + \gamma r'\cos\theta = 2\frac{h_o h_i}{h_o+h_i}$$

Hence

$$p = \frac{6\mu\omega r_m}{\gamma} \frac{\sin\theta}{\cos^2\theta} \frac{h-h_o}{h^2 h_o^2} (\frac{h_o+h}{h_o+h_i} h_o h_i - hh_o)$$

or

$$p = 3\mu\omega C R_m \epsilon \sin\theta \frac{(r_o-r)(r-r_i)}{h_m h^2} \qquad (9)$$

5

where $h_m = (h_o + h_i)/2$.

In [11] where radial variations in h are neglected and the film thickness expression is:

$$h = h_m = C + \gamma r_m \cos\theta$$

the pressure is given by

$$p = \frac{3\mu\omega CR_m \epsilon \sin\theta}{h_m^3}[\frac{1}{4}(r_o - r_i)^2 - (r - r_m)^2]$$

which can be rearranged in the form

$$p_{ap} = 3\mu\omega CR_m \epsilon \sin\theta \ \frac{(r_o - r)(r - r_i)}{h_m^3} \tag{10}$$

The symbol p_{ap} is used in (10) to indicate that the pressure in [11] is only an approximation resulting from the omission of radial variations in h. The accurate pressure given by (9) is related to the approximate pressure of Eq. (10) by

$$p = p_{ap}(\frac{h_m}{h})^2 \tag{11}$$

The film thickness, h, given by Eq. (2) can be written in the form

$$h = C(1 + \epsilon R\cos\theta) \tag{12}$$

The mean thickness, h_m, is

6

$$h_m = C(1 + \epsilon R_m \cos\theta) \qquad\qquad (13)$$

Hence, from (11) it is clear that for $\cos\theta > 0$, p_{ap} underestimates the pressure at any $R > R_m$ and overestimates the pressure at any $R < R_m$. For $\cos\theta < 0$, p_{ap} is an overestimation when $R > R_m$ and an underestimation of the accurate pressure when $R < R_m$. The approximate pressure p_{ap} is antisymmetric about the line BB which connects the highest and lowest points of the seal (see Figure 1), but the ratio h_m/h is symmetric about that line. Hence, the accurate pressure p is from (11) also antisymmetric about line BB.

In the absence of an hydrostatic component this will mean negative pressures in the diverging clearance where $dh/d\theta > 0$. For the narrow seal approximation cavitation is assumed to occur in this section of the seal [11] and the pressure is assumed to be zero (half Sommerfeld condition). When the hydrostatic pressure component does exist the extent of cavitation is dependent on the pressure differential across the seal boundaries. The cavitation zone decreases as the sealed pressure increases until a full fluid film condition is reached.

The two extreme cases, namely, the half Sommerfeld condition for cavitating flow and the full fluid film condition for high pressure seals, will now be considered.

Cavitating Flow:

Axial Force:

In the case of a very small pressure differential across the seal boundaries the axial force is

$$F = \int_0^\pi \int_{r_i}^{r_o} p r \, dr \, d\theta \qquad (14)$$

Substituting Eqs. (12) and (13) into Eq. (9) we have

$$p = 3\mu\omega\left(\frac{r_o}{C}\right)^2 R_m (1-R)(R-R_i)\frac{\epsilon\sin\theta}{(1 + \epsilon R_m\cos\theta)(1 + \epsilon R\cos\theta)^2} \qquad (15)$$

Neglecting curvature effects and substituting the pressure given by (15), Eq. (14) becomes

$$F = 3\mu\omega\left(\frac{r_o}{C}\right)^2 r_m^2 \int_0^\pi \int_{R_i}^1 \frac{(1-R)(R-R_i)\epsilon\sin\theta}{(1+\epsilon R\cos\theta)^2(1+\epsilon R_m\cos\theta)} \, dR \, d\theta \qquad (16)$$

The integration over R can be performed by parts noting that

$$\frac{d}{dR}(1-R)(R-R_i) = 2(R_m-R) \qquad (17)$$

Hence

$$\int_{R_i}^1 \frac{(1-R)(R-R_i)}{(1+\epsilon R\cos\theta)^2} \, dR = - \left. \frac{(1-R)(R-R_i)}{\epsilon\cos\theta(1+\epsilon R\cos\theta)}\right|_{R_i}^1 +$$
$$+ \frac{2}{\epsilon\cos\theta}\int_{R_i}^1 \frac{R_m - R}{1 + \epsilon R\cos\theta} \, dR \qquad (18)$$

The first term on the right hand side of (18) vanishs on both limits of the integration. The second term yields

$$\frac{2}{\epsilon\cos\theta}\int_{R_i}^1 \frac{R_m-R}{1+\epsilon R\cos\theta} \, dR = \frac{2}{\epsilon\cos\theta}\left\{\frac{R_m}{\epsilon\cos\theta}\ln(1+\epsilon R\cos\theta)\right.$$

$$\left.- \frac{1}{(\epsilon\cos\theta)^2}[1 + \epsilon R\cos\theta - \ln(1+\epsilon R\cos\theta)]\right\}\Bigg|_{R_i}^1 =$$

$$= \frac{2}{(\epsilon\cos\theta)^3}[(1+\epsilon R_m\cos\theta)\ln\frac{1+\epsilon\cos\theta}{1+\epsilon R_i\cos\theta} - (1-R_i)\epsilon\cos\theta] \tag{19}$$

Substituting into (16) yields

$$F = 6\mu\omega(\frac{r_o}{C})^2 r_m^2 \int_o^\pi [\frac{\epsilon\sin\theta}{(\epsilon\cos\theta)^3} \ln\frac{1+\epsilon\cos\theta}{1+\epsilon R_i\cos\theta}$$

$$- (1-R_i)\frac{\epsilon\sin\theta}{(\epsilon\cos\theta)^2(1 + \epsilon R_m\cos\theta)}]d\theta \tag{20}$$

Defining the integrals

$$I_1(R,\theta) = \int\frac{\epsilon\sin\theta}{(\epsilon\cos\theta)^3} \ln(1 + \epsilon R\cos\theta)d\theta \tag{21}$$

and

$$I_2(\theta) = \int\frac{\epsilon\sin\theta}{(\epsilon\cos\theta)^2(1 + \epsilon R_m\cos\theta)} d\theta \tag{22}$$

and using the substitution $u=\epsilon\cos\theta$, we find [13]:

$$I_1(R,\theta) = \frac{\ln(1+\epsilon R\cos\theta)}{2(\epsilon\cos\theta)^2} + \frac{R}{2\epsilon\cos\theta} - \frac{R^2}{2} \ln\frac{1 + \epsilon R\cos\theta}{\epsilon\cos\theta} \tag{23}$$

$$I_2(\theta) = \frac{1 + \epsilon R_m\cos\theta}{\epsilon\cos\theta} - R_m\ln\frac{1 + \epsilon R_m\cos\theta}{\epsilon\cos\theta} \tag{24}$$

Substituting Eqs. (23) and (24) into Eq. (20) we have for the axial force

$$\bar{F} = R_m^2 J_1(\theta)\Big|_o^\pi \tag{25}$$

9

where

$$J_1(\theta) = I_1(1,\theta) - I_1(R_i,\theta) - (1-R_i)I_2(\theta) \qquad (26)$$

and $\overline{F}$ is a dimensionless force defined by

$$\overline{F} = \frac{F}{6\mu\omega(\frac{r_o}{C})^2 r_o^2}$$

$I_1(1,\theta)$ and $I_1(R_i,\theta)$ are obtained from Eq. (23) by substituting $R=1$ and $R=R_i$, respectively. After some algebra $J_1(\theta)$ is obtained as follows:

$$J_1(\theta) = \frac{1}{2(\epsilon\cos\theta)^2} \ln \frac{1+\epsilon\cos\theta}{1+\epsilon R_i\cos\theta} - \frac{1-R_i}{2\epsilon\cos\theta} - \frac{1}{2} \ln \frac{1+\epsilon\cos\theta}{1+\epsilon R_m\cos\theta}$$
$$+ \frac{R_i^2}{2} \ln \frac{1+\epsilon R_i\cos\theta}{1+\epsilon R_m\cos\theta} \qquad (27)$$

It is noted that $J_1(\theta)$ as given in (27) is bounded at $\theta=\pi/2$ and hence, F is integrable over the interval $0<\theta<\pi$. This can be readily shown by expanding the first logarithmic term of (27) in the form

$$\ln(1+x) = x - \frac{x^2}{2} + \frac{x^3}{3} + \dots \qquad (28)$$

As $\theta\to\pi/2$, $\cos\theta\to0$, hence orders of $(\cos\theta)^2$ and higher can be neglected, and by (28) we have

$$\lim_{\theta\to\pi/2} [\frac{1}{2(\epsilon\cos\theta)^2} \ln \frac{1+\epsilon\cos\theta}{1+\epsilon R_i\cos\theta} - \frac{1-R_i}{2\epsilon\cos\theta}] = \frac{R_i^2-1}{4}$$

Finally, the dimensionless axial force is by (25) and (27)

10

$$\bar{F} = \left[\frac{1-R_i}{\epsilon} - \frac{1}{2\epsilon^2}\left(\ell n\frac{1+\epsilon}{1-\epsilon} - \ell n\frac{1+\epsilon R_i}{1-\epsilon R_i}\right) + \frac{1}{2}\left(\ell n\frac{1+\epsilon}{1-\epsilon} - \ell n\frac{1+\epsilon R_m}{1-\epsilon R_m}\right)\right.$$

$$\left. + \frac{R_i^2}{2}\left(\ell n\frac{1+\epsilon R_m}{1-\epsilon R_m} - \ell n\frac{1+\epsilon R_i}{1-\epsilon R_i}\right)\right]R_m^2 \tag{29}$$

Eq. (29) gives the axial force over the complete range of misalignment that is, from aligned faces at $\epsilon=0$ to touch down at $\epsilon=1$.

A simpler expression for $\bar{F}$ can be derived for small tilts by using the expansion

$$\ell n\frac{1+x}{1-x} = 2\left(x + \frac{x^3}{3} + \frac{x^5}{5} + \ldots\right) \tag{30}$$

With this expansion Eq. (29) can be rearranged in the form

$$\bar{F} = \left\{\frac{1-R_i}{\epsilon} - \frac{1}{\epsilon^2}\left[\epsilon(1-R_i) + \frac{\epsilon^3}{3}(1-R_i^3) + \frac{\epsilon^5}{5}(1-R_i^5) + \ldots\right]\right.$$

$$+ \left[\epsilon(1-R_m) + \frac{\epsilon^3}{3}(1-R_m^3) + \ldots\right]$$

$$\left. + R_i^2\left[\epsilon(R_m-R_i) + \frac{\epsilon^3}{3}(R_m^3-R_i^3) + \ldots\right]\right\}R_m^2 \tag{31}$$

Neglecting terms of order ϵ^2 and higher and noting that

$$1-R_m = R_m-R_i = \frac{1}{2}(1-R_i) \tag{32}$$

we have for the axial force at very small tilts

$$\bar{F} = \left[-\frac{\epsilon}{3}(1-R_i^3) + \frac{\epsilon}{2}(1-R_i)(1+R_i^2)\right]R_m^2$$

which reduces to

$$\overline{F} = \frac{\epsilon}{6}(1-R_i)^3 R_m^2 \tag{33}$$

The expression for the axial force given by (33) is the same as the one obtained in [11] where very small tilts are assumed. Hence, when dealing with small ϵ values the omission of radial variations in h is an acceptable approximation.

When the sealing surfaces come into contact at $\epsilon=1$, the dimensionless axial force in (29) becomes

$$\overline{F} = [1-R_i + \frac{1-R_i^2}{2}(\ln\frac{1+R_i}{1-R_i} + \ln\frac{1-R_m}{1+R_m}) + \lim_{\epsilon\to 1} \frac{1-\epsilon^2}{2\epsilon^2} \ln(1-\epsilon)]R_m^2$$

Using Eq. (32) and noting that

$$\lim_{\epsilon\to 1} \ln(1-\epsilon)^{(1-\epsilon^2)/2\epsilon^2} = 0$$

we have at $\epsilon=1$

$$\overline{F}_{\epsilon=1} = (1-R_i)(1 + R_m\ln\frac{R_m}{1+R_m})R_m^2 \tag{34}$$

Restoring Moment:

The restoring moment about the x axis (Figure 1) is

$$M_x = - \int_o^\pi \int_{r_i}^{r_o} pr^2\cos\theta\, dr d\theta$$

12

Neglecting curvature effects this becomes

$$M_x = - r_m^2 \iint p\cos\theta \, dr \, d\theta \tag{35}$$

The sign convention in (35) assures that a restoring moment will have a positive value. Using Eqs. (15), (18), and (19), we have

$$M_x = - 6\mu\omega\left(\frac{r_0}{C}\right)^2 r_m^3 \frac{1}{\varepsilon} \int_o^\pi \left[\frac{\varepsilon\sin\theta}{(\varepsilon\cos\theta)^2} \ln\frac{1+\varepsilon\cos\theta}{1+\varepsilon R_i\cos\theta}\right.$$

$$\left. - (1-R_i)\frac{\varepsilon\sin\theta}{\varepsilon\cos\theta(1+\varepsilon R_m\cos\theta)}\right] d\theta$$

Defining the integrals

$$I_3(R,\theta) = \int \frac{\varepsilon\sin\theta}{(\varepsilon\cos\theta)^2} \ln(1+\varepsilon R\cos\theta) \, d\theta \tag{36}$$

and

$$I_4(\theta) = \int \frac{\varepsilon\sin\theta \, d\theta}{\varepsilon\cos\theta(1+\varepsilon R_m\cos\theta)} \tag{37}$$

we find

$$I_3(R,\theta) = \frac{\ln(1+\varepsilon R\cos\theta)}{\varepsilon\cos\theta} + R\ln\frac{1+\varepsilon R\cos\theta}{\varepsilon\cos\theta} \tag{38}$$

$$I_4(\theta) = \ln\frac{1+\varepsilon R_m\cos\theta}{\varepsilon\cos\theta} \tag{39}$$

and the nondimensional restoring moment becomes

13

$$\overline{M}_{(x)} = -\frac{R_m^3}{\varepsilon} J_2(\theta) \Big|_0^\pi \qquad (40)$$

where

$$J_2(\theta) = I_3(1,\theta) - I_3(R_i,\theta) - (1-R_i)I_4(\theta) \qquad (41)$$

and

$$\overline{M}_x = \frac{M_x}{6\mu\omega(\frac{r_o}{C})^2 r_o^3} $$

After some algebra, $J_2(\theta)$ becomes

$$J_2(\theta) = \frac{1}{\varepsilon\cos\theta} \ln \frac{1+\varepsilon\cos\theta}{1+\varepsilon R_i\cos\theta} + \ln \frac{1+\varepsilon\cos\theta}{1+\varepsilon R_m\cos\theta} - R_i \ln \frac{1+\varepsilon R_i\cos\theta}{1+\varepsilon R_m\cos\theta} \qquad (42)$$

Expanding the first logarithmic term in (42) by the serie of (28), yields

$$\lim_{\theta\to\pi/2} \left(\frac{1}{\varepsilon\cos\theta} \ln \frac{1+\varepsilon\cos\theta}{1+\varepsilon R_i\cos\theta}\right) = 1-R_i$$

Hence, $M_{(x)}$ is integrable over the interval $0<\theta<\pi$ and the nondimensional restoring moment is

$$\overline{M}_x = [\frac{1}{\varepsilon^2} \ln \frac{1-\varepsilon^2}{1-\varepsilon^2 R_i^2} + \frac{1}{\varepsilon}(\ln\frac{1+\varepsilon}{1-\varepsilon} - \ln\frac{1+\varepsilon R_m}{1-\varepsilon R_m})$$
$$+ \frac{R_i}{\varepsilon}(\ln\frac{1+\varepsilon R_m}{1-\varepsilon R_m} - \ln\frac{1+\varepsilon R_i}{1-\varepsilon R_i})]R_m^3 \qquad (43)$$

For small ε, if we use the expansion

14

$$\ln(1-x) = -(x + \frac{x^2}{2} + \frac{x^3}{3} + \ldots) \tag{44}$$

and the one given by (30), $\overline{M}_{(x)}$ can be expanded in the form

$$\overline{M}_x = \{ -\frac{1}{\epsilon^2}[\epsilon^2(1-R_i^2) + \frac{\epsilon^4}{2}(1-R_i^4) + \ldots] + \frac{2}{\epsilon}[\epsilon(1-R_m) + \frac{\epsilon^3}{3}(1-R_m^3) + \ldots]$$
$$+ \frac{2R_i}{\epsilon}[\epsilon(R_m-R_i) + \frac{\epsilon^3}{3}(R_m^3-R_i^3) + \ldots] \} R_m^3 \tag{45}$$

which, after neglecting high orders of ϵ, becomes for very small tilts

$$\overline{M}_x = \frac{\epsilon^2}{6} R_m^4 (1-R_i)^3 \tag{45}$$

At $\epsilon=1$ the nondimensional restoring moment is

$$\overline{M}_{x_{\epsilon=1}} = [R_i \ln \frac{1+R_m}{R_m} - \ln R_m(1+R_m)] R_m^3 \tag{46}$$

Transverse Moment:

The moment about the z axis (Figure 1) is

$$M_z = \int_o^\pi \int_{r_i}^{r_o} pr^2 \sin\theta dr d\theta$$

which after neglecting curvature effects becomes

$$M_z = r_m^2 \int_o^\pi \int_{r_i}^{r_o} p\sin\theta dr d\theta \tag{47}$$

Again, by Eqs. (15), (18), and (19)

15

$$M_z = 6\mu\omega\left(\frac{r_o}{C}\right)^2 r_m^3 \int_0^\pi [\frac{\varepsilon\sin^2\theta}{(\varepsilon\cos\theta)^3} \ln\frac{1+\varepsilon\cos\theta}{1+\varepsilon R_i\cos\theta}$$

$$- (1-R_i)\frac{\varepsilon\sin^2\theta}{(\varepsilon\cos\theta)^2(1+\varepsilon R_m\cos\theta)}]d\theta \qquad (48)$$

Integrating by parts and using I_1 and I_2 as defined in Eqs. (21) and (22) we have

$$\int\frac{\varepsilon\sin^2\theta}{(\varepsilon\cos\theta)^3} \ln(1+\varepsilon R\cos\theta)d\theta = I_1(R,\theta)\sin\theta - \int I_1(R,\theta)\cos\theta d\theta \qquad (49)$$

and

$$\int\frac{\varepsilon\sin^2\theta d\theta}{(\varepsilon\cos\theta)^2(1+\varepsilon R_m\cos\theta)} = I_2(\theta)\sin\theta - \int I_2(\theta)\cos\theta d\theta \qquad (50)$$

On both boundaries of the integration ($\theta=0$ and $\theta=\pi$) $\sin\theta=0$. Hence, substituting Eqs. (49) and (50) into (48) yields

$$M_z = -6\mu\omega\left(\frac{r_o}{C}\right)^2 r_m^3 \int_0^\pi [I_1(1,\theta) - I_1(R_i,\theta) - (1-R_i)I_2(\theta)]\cos\theta d\theta \qquad (51)$$

The sum in the brackets under the integral of Eq. (51) was already found, see Eqs. (26) and (27). Thus, the transverse moment in its dimensionless form can be written as

$$\overline{M}_z = \frac{-R_m^3}{2\varepsilon} \int_0^\pi [\frac{1}{\varepsilon\cos\theta} \ln\frac{1+\varepsilon\cos\theta}{1+\varepsilon R_i\cos\theta} - (1-R_i)$$

$$- \varepsilon\cos\theta(\ln\frac{1+\varepsilon\cos\theta}{1+\varepsilon R_m\cos\theta} + R_i^2\ln\frac{1+\varepsilon R_i\cos\theta}{1+\varepsilon R_m\cos\theta})]d\theta \qquad (52)$$

where

16

$$\overline{M}_z = \frac{M_z}{6\mu\omega(\frac{r_o}{C})^2 r_o^3}$$

From [14] we find

$$\int_o^\pi \frac{\ell n(1+\epsilon R\cos\theta)}{\cos\theta} d\theta = \pi\sin^{-1}(\epsilon R) \tag{53}$$

Also, integrating by parts, we have

$$\int_o^\pi \cos\theta\, \ell n(1+\epsilon R\cos\theta) = \epsilon R \int_o^\pi \frac{\sin^2\theta}{1+\epsilon R\cos\theta} d\theta \tag{54}$$

and from [15]

$$\int_o^\pi \frac{\sin^2\theta}{1+\epsilon R\cos\theta} d\theta = \frac{\pi}{\epsilon^2 R^2}[1 - (1 - \epsilon^2 R^2)^{1/2}] \tag{55}$$

Substituting Eqs. (53), (54), and (55) into Eq. (52) yields after some algebra

$$\overline{M}_z = \{\frac{\pi}{2\epsilon^2}[\sin^{-1}(\epsilon R_i) - \sin^{-1}(\epsilon)] + \frac{\pi}{\epsilon}(1-R_i)(1-\epsilon^2 R_m^2)^{1/2}$$

$$+ \frac{\pi}{2\epsilon}[R_i(1-\epsilon^2 R_i^2)^{1/2} - (1-\epsilon^2)^{1/2}]\}R_m^3 \tag{56}$$

For small tilts we can use the approximations

$$\sin^{-1}(\epsilon R) = \epsilon R + \frac{\epsilon^3 R^3}{2.3} + \ldots$$

and

17

$$(1-\varepsilon^2 R^2)^{\frac{1}{2}} = 1 - \frac{1}{2}\varepsilon^2 R^2$$

Thus, for very small ε Eq. (56) becomes

$$\bar{M}_z = \frac{\pi\varepsilon}{24}(1-R_i)^3 R_m^3 \tag{57}$$

Full Fluid Film:

Under full fluid film condition the hydrodynamic pressure is antisymmetric about the line connecting the highest and lowest points of the seal ring (line BB in Figure 1). This results in a net zero axial force and eliminates the hydrodynamic component of any restoring moment, M_x. However, the transverse moment, M_z, becomes twice its value for the half Sommerfeld condition. Thus, by (56) we have for full fluid film condition

$$\bar{M}_z = \{\frac{\pi}{\varepsilon^2}[\sin^{-1}(\varepsilon R_i) - \sin^{-1}(\varepsilon)] + \frac{2\pi}{\varepsilon}(1-R_i)(1-\varepsilon^2 R_m^2)^{\frac{1}{2}}$$

$$+ \frac{\pi}{\varepsilon}[R_i(1-\varepsilon^2 R_i^2)^{\frac{1}{2}} - (1-\varepsilon^2)^{\frac{1}{2}}]\}R_m^3 \tag{58}$$

and by (57) for very small tilts

$$\bar{M}_z = \frac{\pi\varepsilon}{12}(1-R_i)^3 R_m^3 \tag{59}$$

The hydrostatic pressure in a misaligned seal is symmetric about line BB. Therefore, in contrast to hydrodynamic effects, it does not produce any transverse moment. Hence, this moment, which is shifted 90 degrees from the mis-

18

alignment vector, is entirely due to hydrodynamic effects.

Although leakage was not treated in the case of a cavitating flow, it should be mentioned that under full fluid film conditions the leakage is entirely hydrostatic. This is due to the antisymmetric nature of the hydro-dynamic pressure which results in zero hydrodynamic leakage.

RESULTS AND DISCUSSION

Values of the nondimensional parameters $\bar{F}$, $\bar{M}_x$, $\bar{M}_z$, and the ratio M_z/M_x for the case of cavitating flow (half Sommerfeld condition) are presented in Table I and Figures 2 to 4. These cover the whole range of tilt parameters, from $\epsilon=0$ to $\epsilon=1$.

The axial force and the restoring and transverse moments are greatly influenced by the radius ratio, r_i/r_o. As r_i/r_o decreases the force and moments increase quite rapidly. At a given radius ratio both the axial force and the restoring moment increase with ϵ. An increase in the tilt parameter, $\epsilon = \gamma r_o/C$, is a result of a decrease in the seal clearance C or an increase in the angle of tilt γ. Hence, $d\bar{F}/d\epsilon$ and $d\bar{M}_x/d\epsilon$ are proportional to the axial stiffness dF/dC and to the angular stiffness $dM_x/d\gamma$, respectively. From Table I and Figures 2 and 3 it is seen that decreases in the radius ratio are accompanied by increases in the axial and angular stiffnesses. Also at a given r_i/r_o the axial and angular stiffness increase with increasing tilt parameter ϵ.

An interesting result is the ratio of transverse to restoring moment M_z/M_x. Whenever $\epsilon>0.6$ M_z is smaller than M_x, but, as ϵ decreases, the ratio M_z/M_x increases and becomes larger than 1 for any $\epsilon<0.6$. At $\epsilon=1$, the transverse moment is only about 10 to 20 percent of the restoring moment but becomes about 8 times larger than the restoring moment at $\epsilon=0.1$. These results are true for any r_i/r_o indicating that the center of pressure is not sensitive to the radius ratio and, what is more important, that there is a strong coupling between transverse moment and angular misalignment immediately after the misalignment begins. Such coupling can lead to dynamic instability

wobbling of the primary seal, similar to a whirl in journal bearings.

In the case of a high pressure seal where the full fluid film condition prevails the hydrodynamic components of the axial force and restoring moment vanish but the transverse moment becomes twice its value for the cavitating flow case. The transverse moment vs. tilt parameter for the full film condition is presented in Figure 5.

It is interesting to compare the transverse moment due to hydrodynamic effects with the hydrostatic tilting moment due to the pressure difference across the seal boundaries. These two moments are 90 degrees apart from each other and therefore the problem of dynamic instability and wobbling in high pressure seals is similar to that occuring in low pressure seals with cavitation.

As an example, a seal having the following dimensions and operating conditions was chosen:

Outer radius, r_o, cm 5

Radius ratio, r_i/r_o 0.9

Mean radius, r_m, cm 4.75

Seal Clearance, C, cm 0.0025

Shaft speed, n, rpm 1000

Fluid viscosity, μ, N-sec/m^2 . . . . 1.72 10^{-3}

Pressure differential, Δp, N/m^2 . . . . 10^6

In [12] a hydrostatic tilting moment of 430 N-cm is found for that seal when $\varepsilon=1$. The hydrodynamic transverse moment at the same tilt parameter and full fluid film condition is 536 N-cm, and would be even higher for smaller

seal clearances C without affecting the hydrostatic tilting moment. Hence, the hydrodynamic transverse moment, which was overlooked in the past, is a significant factor in both low and high pressure seals and clearly plays an important role in radial face seal operation.

REFERENCES

1. Denny, D. F.: Some measurements of fluid pressures between plane parallel thrust surfaces with special reference to radial-face seals. Wear, Vol. 4, 1961, pp. 64-83.

2. Sneck, H. J.: The effect of geometry and inertia on face seal performance - laminar flow. J. Lub. Tech., Trans. ASME, Series F, Vol. 90, No. 2, April 1968, pp. 333-341.

3. Pape, J. G.: Fundamental research on radial face seals. ASLE Trans., Vol. 11, No. 4, October 1968, pp. 302-309.

4. Kuzma, D. C.: Theory of the mechanism of sealing with application to face seals. J. Lub. Tech., Trans. ASME, Series F, Vol. 91, No. 4, October 1969, pp. 704-712.

5. Stanghan-Batch, B. and Iny, E. H.: A hydrodynamic theory of radial face mechanical seals. J. Mech. Eng. Sci., Vol. 15, No. 1, February 1973, pp. 17-24.

6. Anno, J. N., Walowit, J. A., and Allen, C. M.: Microasperity lubrication. J. Lub. Tech., Trans. ASME, Series F, Vol. 90, No. 2, April 1968, pp. 351-355.

7. Orcutt, F. K.: An investigation of the operation and failure of mechanical face seals. J. Lub. Tech., Trans. ASME, Series F, Vol. 91, No. 4, October 1969, pp. 713-725.

8. Li, Chin-Hsiu: Thermal deformation in a mechanical face seal. ASLE Trans., Vol. 19, No. 2, April 1976, pp. 146-152.

9. Kilaparti, S. R. and Burton, R. A.: Pressure distribution for patch-like contact in seals with frictional heating, thermal expansion, and wear. J. Lub. Tech., Trans. ASME, Series F, Vol. 98, No. 4, October 1976, pp. 569-601.

23

10. Kupperman, D. S.: Dynamic tracking of noncontacting face seals. *ASLE Trans.*, Vol. 18, No. 4, October 1975, pp. 306-311.

11. Ludwig, L. P. and Gordon, P. A.: Face seal lubrication. II. Theory of response to angular misalignment. NASA TN D-8102, March 1976.

12. Etsion, I.: Nonaxisymmetric incompressible hydrostatic pressure effects in radial face seals. NASA TN D-8343, November 1976.

13. Dwight, H. B.: *Tables of Integrals and Other Mathematical Data*. The Macmillan Co., 1957.

14. Gradshteyn, I. S. and Ryzhik, I. M.: *Tables of Integrals Series and Products*. Academic Press, 1965.

15. Booker, J. F.: A table of the journal-bearing integral. *J. Basic Eng.*, Trans. ASME, Series D, Vol. 87, June 1965, pp. 533-535.

r_i/r_o	ε	$\bar{F}$	$\bar{M}_x$	$\bar{M}_z$	M_z/M_x
0.82	0.1	0.110E-03	0.887E-05	0.773E-04	0.869E 01
	0.2	0.231E-03	0.374E-04	0.160E-03	0.429E 01
	0.3	0.377E-03	0.917E-04	0.257E-03	0.280E 01
	0.4	0.571E-03	0.185E-03	0.376E-03	0.203E 01
	0.5	0.850E-03	0.345E-03	0.537E-03	0.156E 01
	0.6	0.130E-02	0.631E-03	0.770E-03	0.122E 01
	0.7	0.210E-02	0.119E-02	0.115E-02	0.962E 00
	0.8	0.380E-02	0.248E-02	0.185E-02	0.747E 00
	0.9	0.876E-02	0.645E-02	0.355E-02	0.550E 00
	1.0	0.531E-01	0.447E-01	0.124E-01	0.278E 00
0.85	0.1	0.490E-04	0.419E-05	0.354E-04	0.845E 01
	0.2	0.103E-03	0.177E-04	0.737E-04	0.417E 01
	0.3	0.170E-03	0.435E-04	0.118E-03	0.272E 01
	0.4	0.259E-03	0.885E-04	0.174E-03	0.197E 01
	0.5	0.390E-03	0.167E-03	0.251E-03	0.150E 01
	0.6	0.604E-03	0.311E-03	0.365E-03	0.117E 01
	0.7	0.100E-02	0.603E-03	0.555E-03	0.921E 00
	0.8	0.191E-02	0.131E-02	0.927E-03	0.708E 00
	0.9	0.481E-02	0.373E-02	0.190E-02	0.511E 00
	1.0	0.413E-01	0.364E-01	0.863E-02	0.237E 00
0.90	0.1	0.153E-04	0.138E-05	0.114E-04	0.823E 01
	0.2	0.324E-04	0.584E-05	0.237E-04	0.406E 01
	0.3	0.535E-04	0.145E-04	0.382E-04	0.264E 01
	0.4	0.822E-04	0.297E-04	0.567E-04	0.191E 01
	0.5	0.125E-03	0.566E-04	0.824E-04	0.145E 01
	0.6	0.198E-03	0.107E-03	0.121E-03	0.113E 01
	0.7	0.339E-03	0.215E-03	0.189E-03	0.880E 00
	0.8	0.679E-03	0.491E-03	0.329E-03	0.669E 00
	0.9	0.192E-02	0.157E-02	0.736E-03	0.470E 00
	1.0	0.286E-01	0.263E-01	0.502E-02	0.191E 00
0.92	0.1	0.801E-05	0.738E-06	0.601E-05	0.814E 01
	0.2	0.170E-04	0.313E-05	0.125E-04	0.401E 01
	0.3	0.281E-04	0.776E-05	0.203E-04	0.261E 01
	0.4	0.433E-04	0.160E-04	0.301E-04	0.189E 01
	0.5	0.664E-04	0.306E-04	0.439E-04	0.143E 01
	0.6	0.106E-03	0.585E-04	0.652E-04	0.111E 01
	0.7	0.183E-03	0.118E-03	0.102E-03	0.864E 00
	0.8	0.376E-03	0.277E-03	0.181E-03	0.653E 00
	0.9	0.112E-02	0.933E-03	0.423E-03	0.453E 00
	1.0	0.232E-01	0.217E-01	0.368E-02	0.170E 00

25

Table I. - Misaligned-Seal Performance Parameters (cavitating flow)

| r_i/r_o	ε	$\bar{F}$	$\bar{M}_x$	$\bar{M}_z$	M_z/M_x
0.94	0.1	0.345E-05	0.325E-06	0.262E-05	0.806E 01
	0.2	0.731E-05	0.138E-05	0.547E-05	0.397E 01
	0.3	0.121E-04	0.342E-05	0.884E-05	0.258E 01
	0.4	0.188E-04	0.707E-05	0.132E-04	0.187E 01
	0.5	0.290E-04	0.136E-04	0.193E-04	0.142E 01
	0.6	0.465E-04	0.263E-04	0.288E-04	0.110E 01
	0.7	0.817E-04	0.538E-04	0.457E-04	0.849E 00
	0.8	0.172E-03	0.129E-03	0.824E-04	0.637E 00
	0.9	0.546E-03	0.463E-03	0.202E-03	0.436E 00
	1.0	0.177E-01	0.168E-01	0.245E-02	0.146E 00
0.96	0.1	0.104E-05	0.100E-06	0.800E-06	0.798E 01
	0.2	0.222E-05	0.426E-06	0.167E-05	0.393E 01
	0.3	0.368E-05	0.106E-05	0.271E-05	0.255E 01
	0.4	0.572E-05	0.220E-05	0.405E-05	0.184E 01
	0.5	0.887E-05	0.426E-05	0.595E-05	0.140E 01
	0.6	0.144E-04	0.828E-05	0.894E-05	0.108E 01
	0.7	0.256E-04	0.172E-04	0.143E-04	0.833E 00
	0.8	0.553E-04	0.425E-04	0.264E-04	0.621E 00
	0.9	0.188E-03	0.163E-03	0.681E-04	0.418E 00
	1.0	0.119E-01	0.116E-01	0.137E-02	0.118E 00
0.98	0.1	0.133E-06	0.131E-07	0.103E-06	0.789E 01
	0.2	0.283E-06	0.555E-07	0.216E-06	0.389E 01
	0.3	0.472E-06	0.139E-06	0.350E-06	0.253E 01
	0.4	0.735E-06	0.288E-06	0.525E-06	0.182E 01
	0.5	0.115E-05	0.562E-06	0.774E-06	0.138E 01
	0.6	0.187E-05	0.110E-05	0.117E-05	0.106E 01
	0.7	0.339E-05	0.232E-05	0.190E-05	0.817E 00
	0.8	0.753E-05	0.590E-05	0.357E-05	0.605E 00
	0.9	0.277E-04	0.245E-04	0.978E-05	0.400E 00
	1.0	0.605E-02	0.595E-02	0.496E-03	0.833E-01
0.99	0.1	0.168E-07	0.167E-08	0.131E-07	0.785E 01
	0.2	0.358E-07	0.708E-08	0.274E-07	0.387E 01
	0.3	0.597E-07	0.177E-07	0.445E-07	0.251E 01
	0.4	0.932E-07	0.369E-07	0.668E-07	0.181E 01
	0.5	0.146E-06	0.721E-07	0.988E-07	0.137E 01
	0.6	0.239E-06	0.142E-06	0.150E-06	0.106E 01
	0.7	0.436E-06	0.302E-06	0.244E-06	0.809E 00
	0.8	0.983E-06	0.779E-06	0.465E-06	0.597E 00
	0.9	0.379E-05	0.337E-05	0.132E-05	0.390E 00
	1.0	0.305E-02	0.302E-02	0.177E-03	0.587E-01

Table I. - Concluded
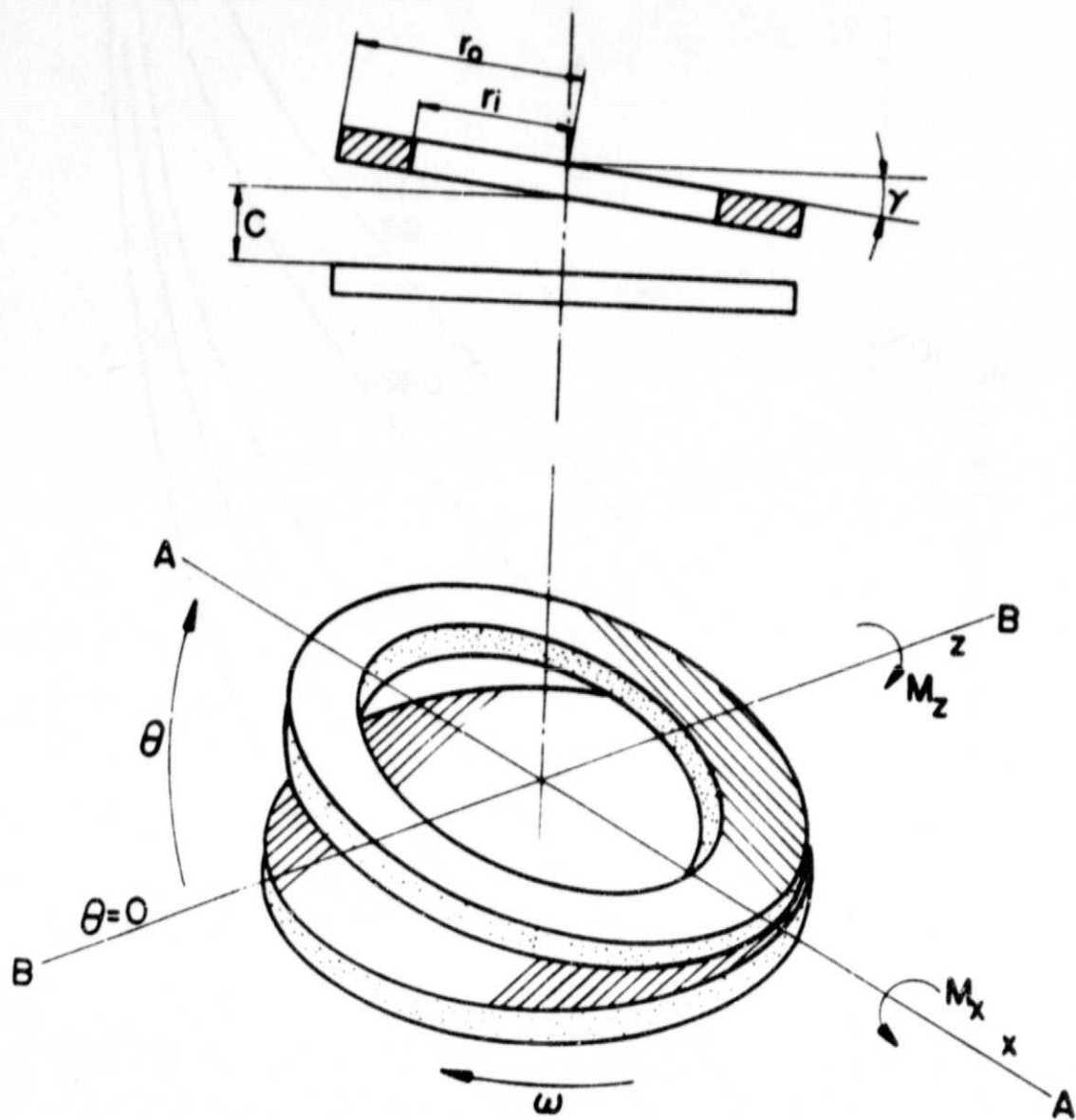
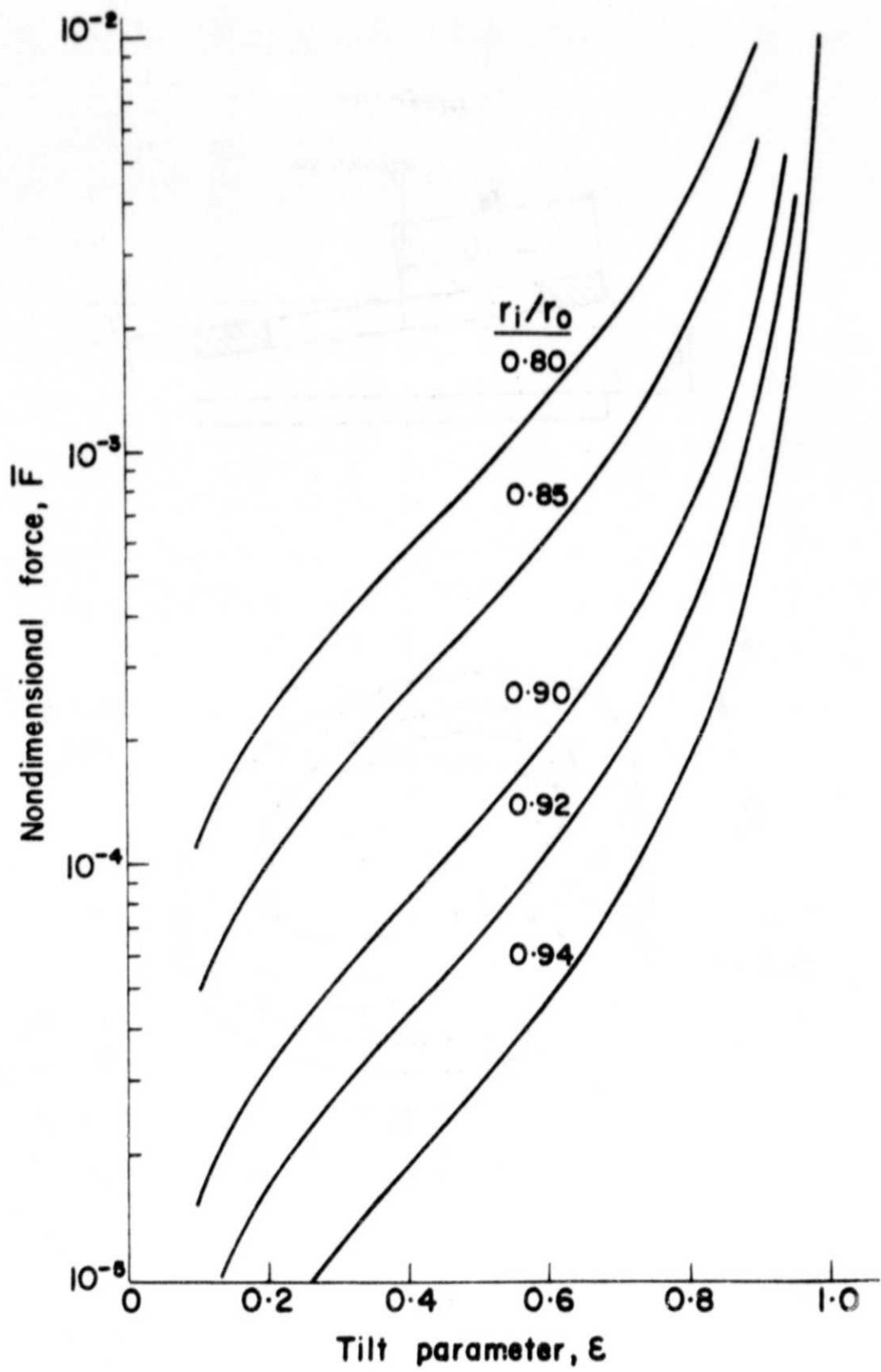Figure 1 - Face seal with angular misalignment.

Figure 2 - Nondimensional force as a function of tilt
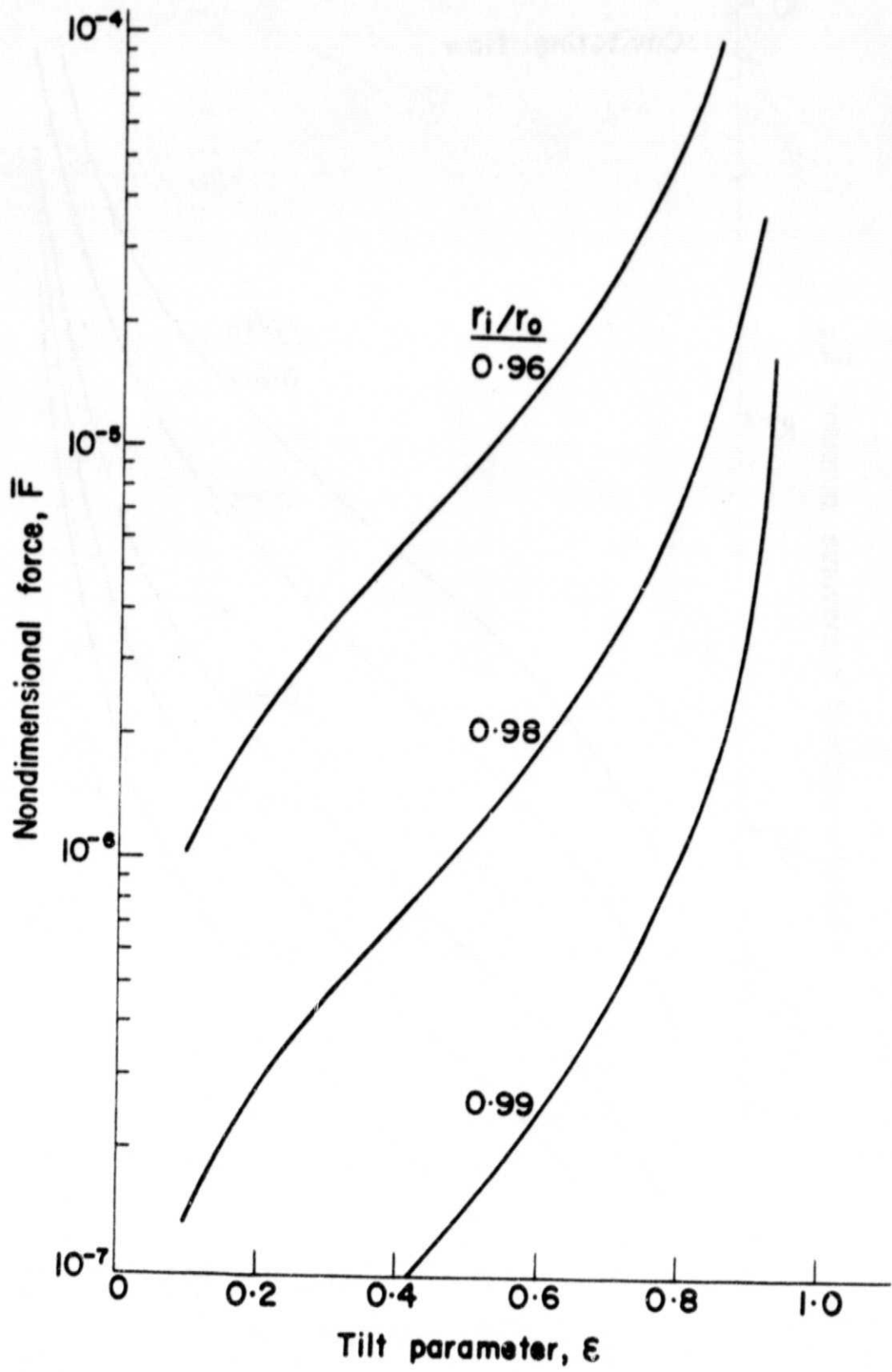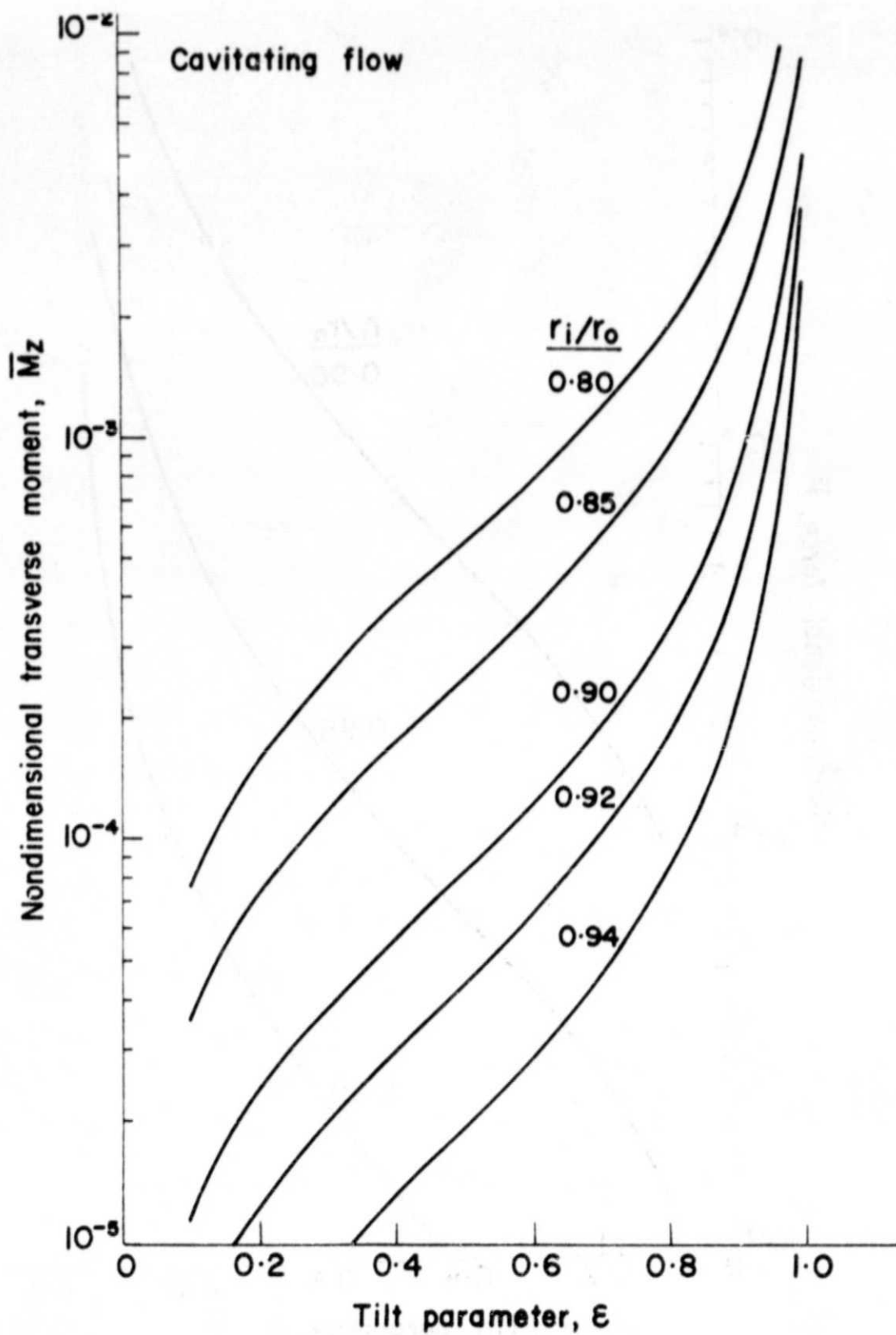parameter for various radius ratios (cavitating flow).

Figure 2 - Concluded.

Figure 3 - Nondimensional transverse moment as a function
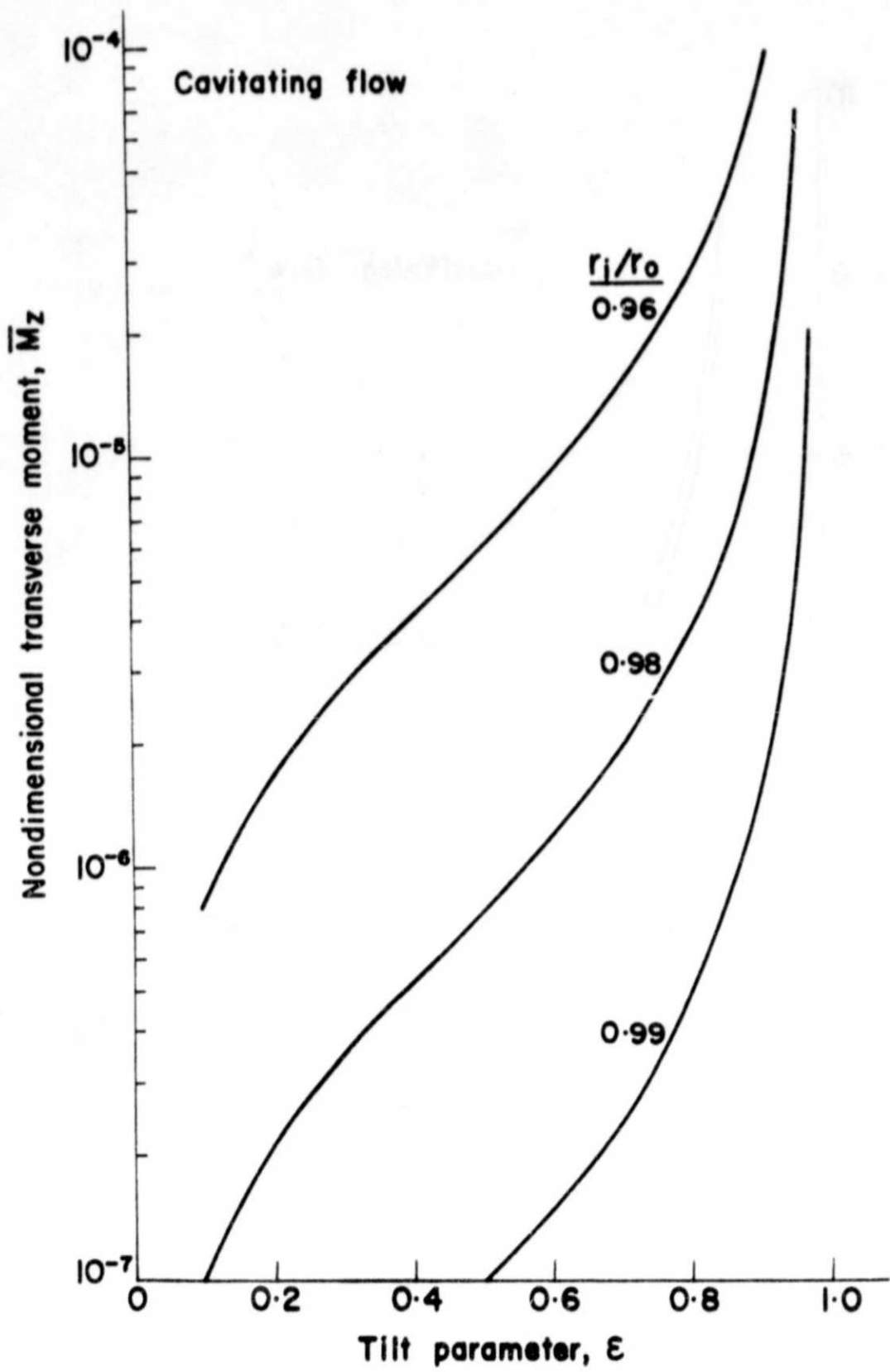of tilt parameter for various radius ratios (cavitating flow).
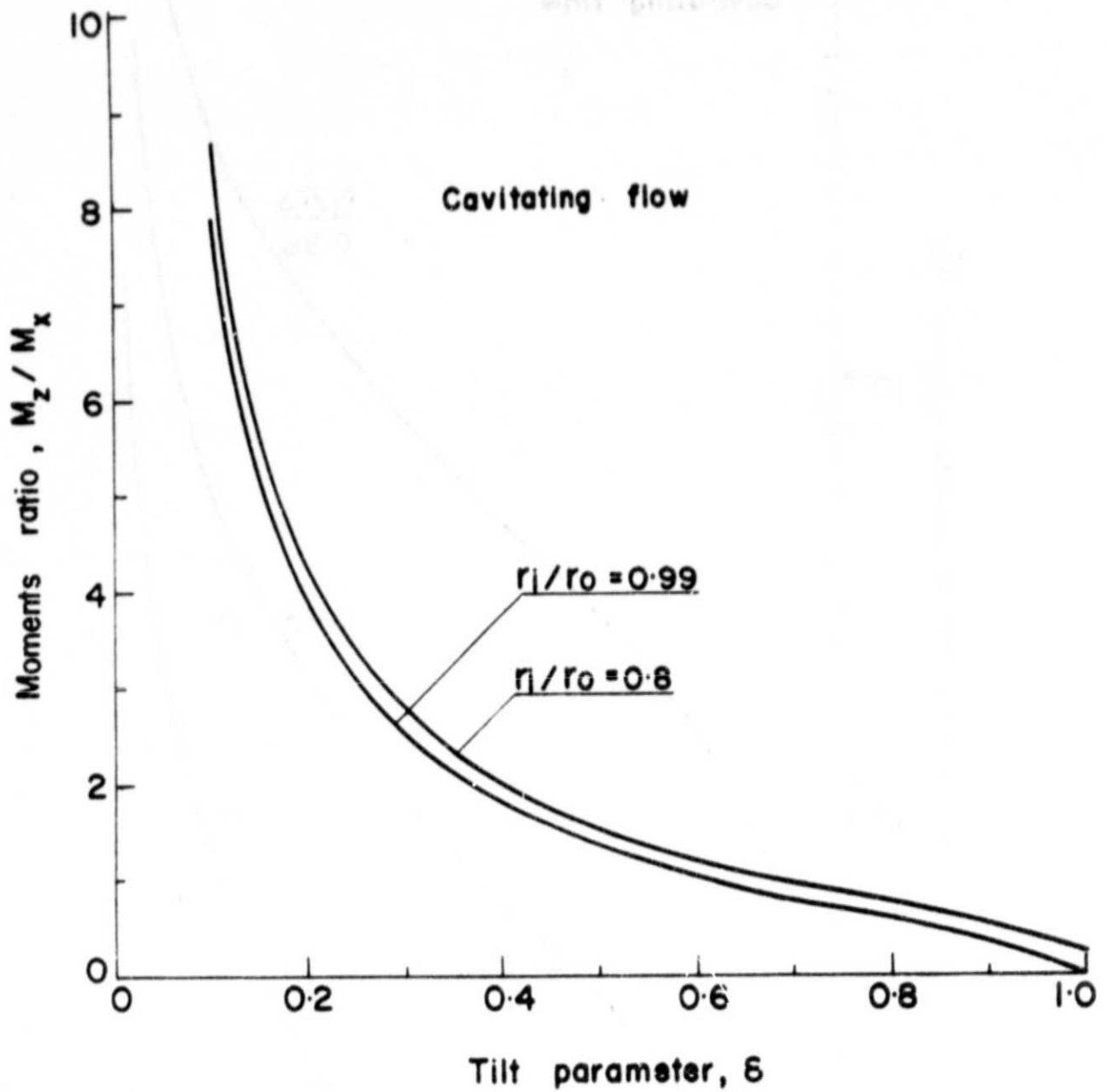
30

Figure 3 - Concluded.

31

Figure 4 - Ratio of transverse to restoring moment as a
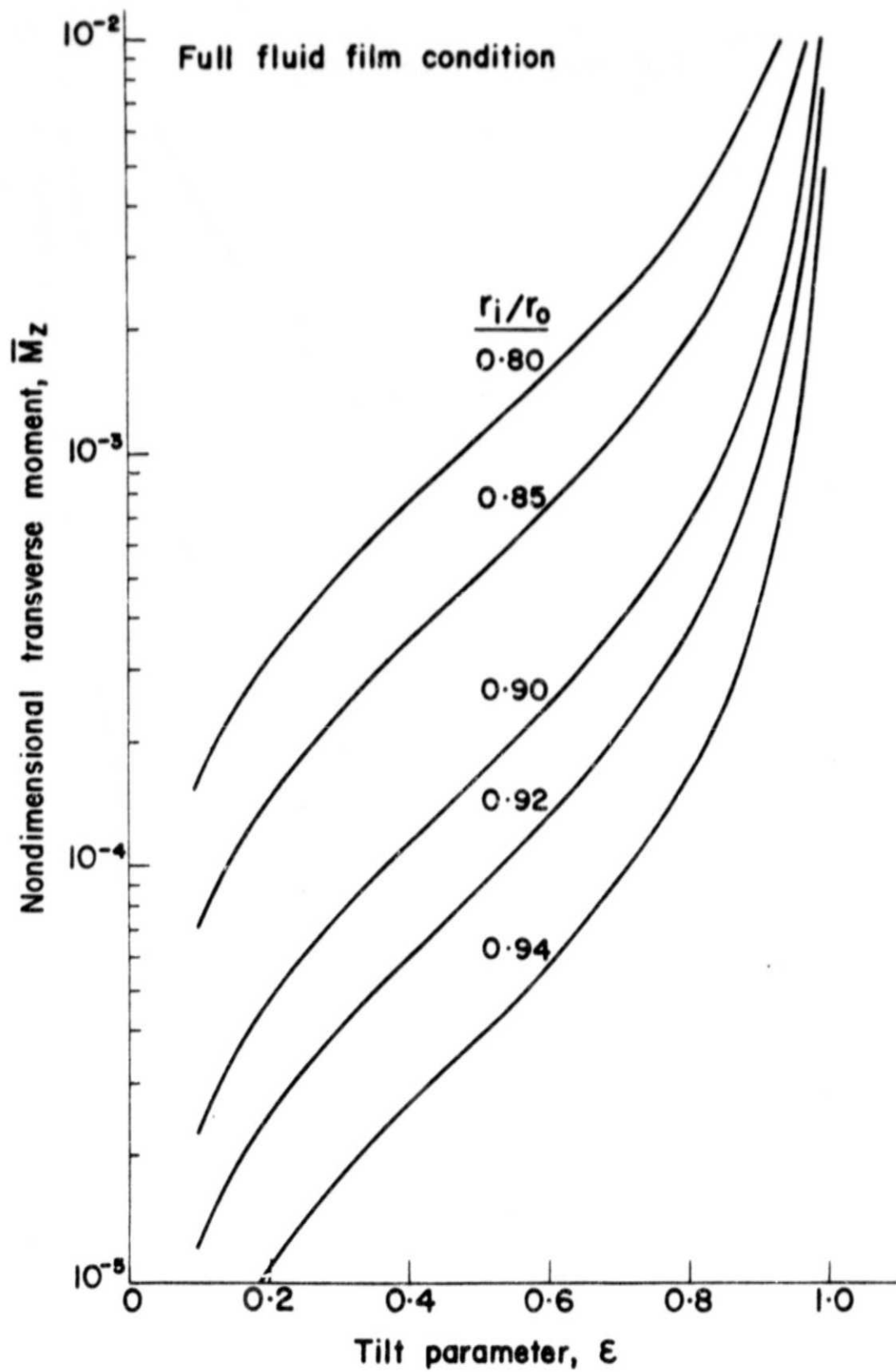function of tilt parameter for various radius ratios
(cavitating flow).

Figure 5 - Nondimensional transverse moment as a function of tilt parameter for varicus radius ratios (full fluid film condition).
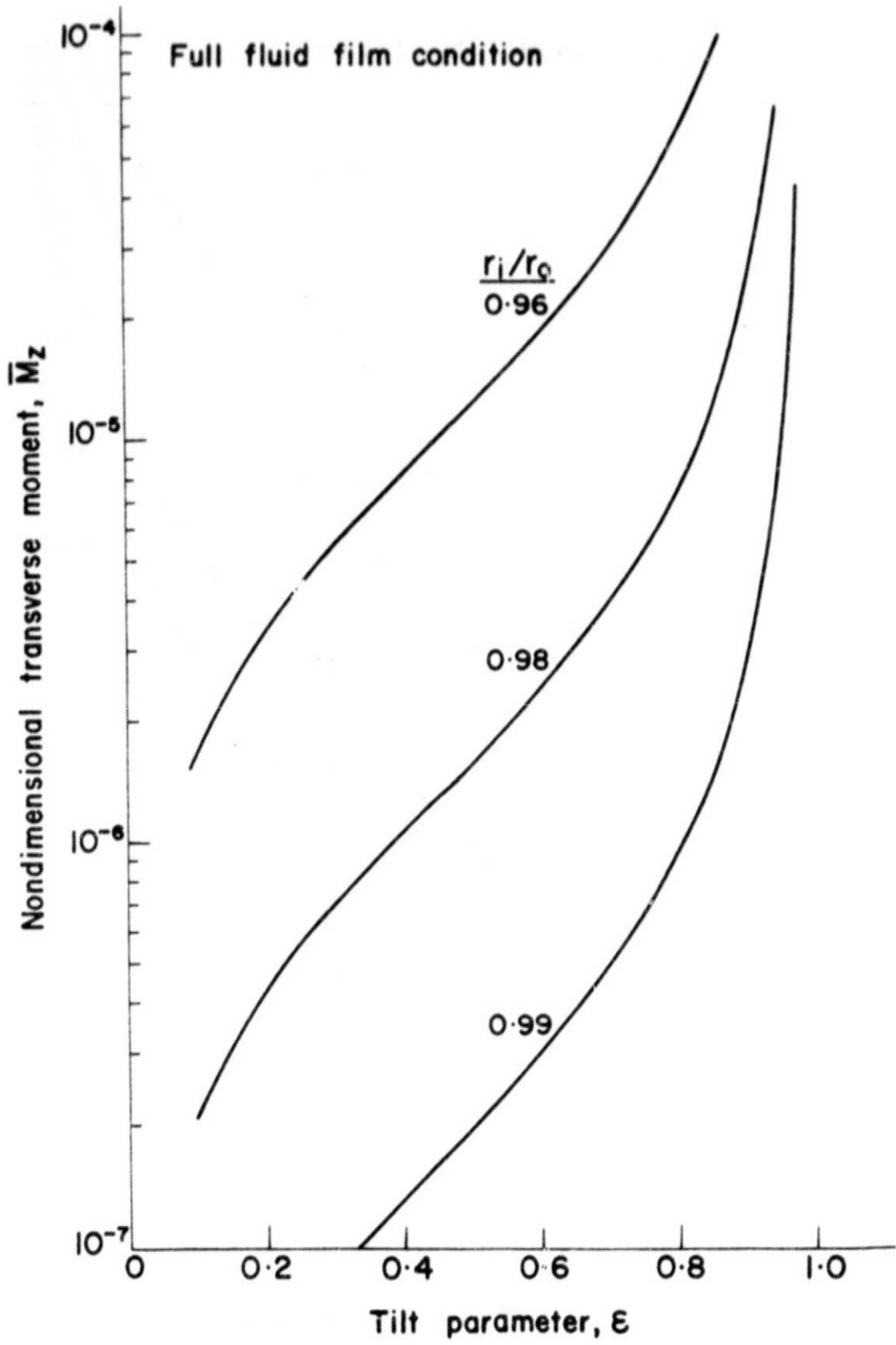
Figure 5 - Concluded.